RSC Advances

PAPER

View Article Online
View Journal | View Issue

Cite this: *RSC Adv.*, 2023, **13**, 21127

Barium silicate nanoparticles, an efficient catalyst for one-pot green synthesis of α-benzyl amino coumarin derivatives as potential chemotherapeutic agents†

Hadi Taghrir,[a] Zeinab Faghih,*[a] Majid Ghashang,*[b] Leila Emami,[a] Shadi Dalili[c] and Soghra Khabnadideh[a]

A new, simple, and efficient method for synthesis of α-benzyl amino coumarin and its derivatives (**1–24**) is described *via* a one-pot, three-component condensation of aromatic aldehydes, amine, and 4-hydroxycoumarin under green chemistry conditions: water as a solvent and $BaSiO_3$ nanoparticles as catalyst. $BaSiO_3$ nanoparticles and all synthesized derivatives were characterized by multiple methods including; XRD, NMR, and FE-SEM. This method which gives higher yields, is also less expensive, and more environmentally friendly compared with other methods in the literature. *In silico* physicochemical and pharmacokinetics analyses were done on all synthesized compounds and indicated that these α-benzyl amino coumarins would be effective scaffolds for the future development of chemotherapeutic agents.

Received 6th February 2023
Accepted 22nd June 2023

DOI: 10.1039/d3ra00796k

rsc.li/rsc-advances

1. Introduction

Recently, 4-hydroxycoumarin and its derivatives have been of great interest due to their special role in natural and synthetic organic chemistry.[1] Furthermore, coumarin is a suitable scaffold for chemical reactions in several studies, due to its hydroxyl and carbonyl groups adjacent to the α-position. Consequently, the 4-hydroxycoumarin and its derivatives have broad spectrum pharmacological properties including: antioxidant,[2] antimicrobial,[3] HIV protease inhibitors,[4] antibacterial,[5] antifungal,[6] antitumor,[7] and anticoagulant[8] activities. Thus, the development of coumarin-containing compounds for drug discovery has recently drawn much attention. α-Benzyl amino coumarins are one of the most useful products resulting from 4-hydroxycoumarin's reactions. These compounds have been developed with various methods such as using: non-ionic surfactant in aqueous media,[9] catalyst-free conditions in dichloromethane,[10] $InCl_3$ in toluene,[11,12] chlorosulfonic acid,[13] TiO_2 nanocatalyst,[14] catalyst-free in ethanol solvent,[15] {[1,4-DHPyrazine][$C(CN)_3$]$_2$} as a new nanostructured molten salt (NMS) catalyst,[16] catalyst-free in CH_2Cl_2 (ref. 17), [Et_3NH][HSO_4] ionic liquid,[18] Fe_3O_4@ZrO_2/SO_4^{-2} heterogeneous nanocatalyst in CH_3CN,[19] β-cyclodextrin based nanosponge in ethanol,[20] free-catalyst in CH_3CN,[21] nano crystalline ZnO,[22] NaOH.[23] However, most of these methods rely on multistep reactions and complex synthetic pathways with prolonged reaction times, low yields, expensive and harsh reaction conditions, as well as toxic catalysts. Thus, the development of new methods without such limitations is of great importance to prepare such heterocycles, found in natural products. Furthermore, multicomponent reactions (MCRs) are generating considerable interest in pharmaceutical chemistry to synthesize diverse structures of bioactive heterocycles, involving three or more reactants in one-pot reactions.[24] Due to non-toxic and unique nature of water, there has been a rapid rise in the use of aqueous environment instead of conventional organic solvents in organic synthesis, especially in the MCRs.

In the present study, due to the importance of α-benzyl amino coumarin scaffolds as a significant class of heterocycles in medicinal chemistry, a new, highly efficient, mild, and eco-friendly synthesis protocol is reported. Condensation between 4-hydroxycoumarin, an aliphatic amine, and a vast range of aromatic aldehydes using barium silicate nanoparticles as a heterogeneous, effective catalyst, is applied to obtain α-benzyl amino coumarin compounds (Scheme 1).

Furthermore, regarding the significant biological profiles of the coumarin-bearing structures, the physicochemical and pharmacokinetic properties of these α-benzyl amino coumarins were examined through *in silico* analysis, to identify them as suitable biological candidates for future evaluations.

[a]*Pharmaceutical Sciences Research Center, Shiraz University of Medical Sciences, Shiraz, Islamic Republic of Iran. E-mail: Faghihl@sums.ac.ir; layafaghih@gmail.com; Fax: +98-7132424126; Tel: +98-7132424127*

[b]*Department of Chemistry, Najafabad Branch, Islamic Azad University, Najafabad, Iran. E-mail: ghashangmajid@pmt.iaun.ac.ir; Fax: +98-3142291016; Tel: +98-3142291004*

[c]*Department of Physical and Environmental Sciences, 1265 Military Trail, Scarborough, ON M1C 1A4, Canada*

† Electronic supplementary information (ESI) available. See DOI: https://doi.org/10.1039/d3ra00796k

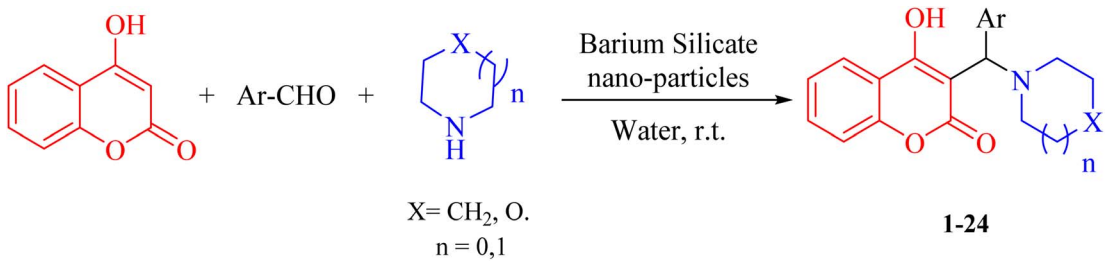

Scheme 1 Synthesis of α-benzyl amino coumarin derivatives.

2. Result and discussion

2.1. Chemistry

In order to determine the crystalline structure and phase composition of the $BaSiO_3$ nanopowder, X-ray diffraction (XRD) analysis using Cu-Kα radiation (Fig. 1). The average size was measured by the Sherer equation by measuring the highest peak (peak appearing at 22.0° (2° theta)); the XRD spectrum was 30 nm.

A particle size distribution diagram was plotted through the data obtained from dynamic light scattering (DLS) analysis and showed the particles were dispersed in the range of 45–140 nm. According to the diagram, the average particle size was 74 nm (Fig. 2). The energy-dispersive X-ray spectroscopy analysis (EDAX) demonstrated the elements in the composition and the weight percentage of each (17.16% Si, 57.35% Ba, and 26.49% O), which confirmed the proposed structure of the composition as $BaSiO_3$. The TEM Photograph displayed unregular and chaotic particles with nanometer size (Fig. 2).

Fig. 3, represented the FT-IR spectra of fresh and recovered $BaSiO_3$ which was used for the evaluation of functional groups presented in the structure of the catalyst. The samples contained metal–oxygen bonds which showed stretching and bending vibrations. The broad adsorption peak which appeared in the 3200–3700 cm^{-1} was corresponded to stretching vibrations of Si–OH and –OH groups presented in $BaSiO_3$ and adsorbed water. The adsorption peaks at 1637, 1448, and 1083 cm^{-1} could be assigned to the presence of Si–O (stretching vibration), and Si–O–Si (asymmetric stretching vibration) bonds. The peaks entered at 798 and 477 cm^{-1} were assigned to be related to Si–O–Ba stretching vibration and Ba–O bonds (Fig. 3).

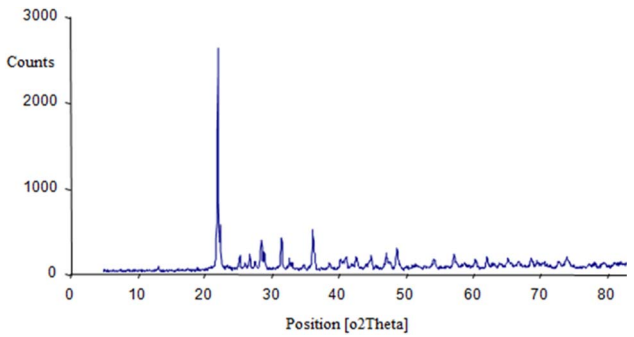

Fig. 1 XRD pattern of $BaSiO_3$ Nanoparticles.

To find the optimal conditions for the synthesis of α-benzyl amino coumarins, the synthesis of 4-hydroxy-3-(phenyl(-piperidine-1-yl)methyl)-2*H*-chromen-2-one (compound $\mathbf{A_1}$), by the reaction of benzaldehyde (1.2 mmol), pyridine (1.2 mmol) and 4-hydroxy-coumarin (1 mmol), was selected as a model reaction.

This reaction was performed in water as a green solvent, as well as in the presence of various organic solvents, using 0.56 mg of barium silicate nanoparticle (1–8) (Table 1).

As seen from the results represented in Table 1, when the model reaction was carried out in the presence of organic solvents, it did not lead to the production of $\mathbf{A_1}$ products but rather led to the formation of 3,3′-(phenyl methylene) bis(4-hydroxy-2*H*-chromen-2-one) ($\mathbf{B_1}$) as a final product. This finding showed that **A** products were only obtained in highly aqueous media. (Scheme 2). The different amounts of barium silicate nanoparticle in the model reaction were also investigated (8–11), which indicated that using 0.28 mg of this catalyst increased the yield of the reaction properly.

Overall, the use of 0.28 mg of designed catalysts in aqueous media was selected as an optimal condition for the model reaction to synthesize various derivatives of α-benzyl amino coumarin compounds using cycloaliphatic amines, different aromatic and aliphatic aldehydes, $\mathbf{A_1}$–$\mathbf{A_{30}}$ (Table 2). As shown in Table 2, unfortunately, the aliphatic aldehydes were unreactive and could not be matched for the given reaction to form targeted molecules. Only aromatic aldehydes generated the desired compounds, $\mathbf{A_1}$–$\mathbf{A_{24}}$ (Table 2).

According to our observations, it is believed that the reaction could be started by the activation of aldehyde using Lewis acid characteristics of $BaSiO_3$ and subsequently formation of iminium ion intermediate **(a)** from the reaction of secondary amine with the activated aldehyde. In addition, 4-hydroxycoumarin could be equilibrated with their enolate ion form **(b)**. The final product would be achieved through the reaction of **a** and **b** and subsequent keto–enol tautomerization as shown in Scheme 3.

The catalyst recyclability also was investigated in the synthesis of product $\mathbf{A_1}$. In each step, the compound separated from the reaction mixture was washed with acetone and dried at 50 °C. The results of 10 recycling and reuse of the catalyst are shown in Fig. 4. The obtained results show the good

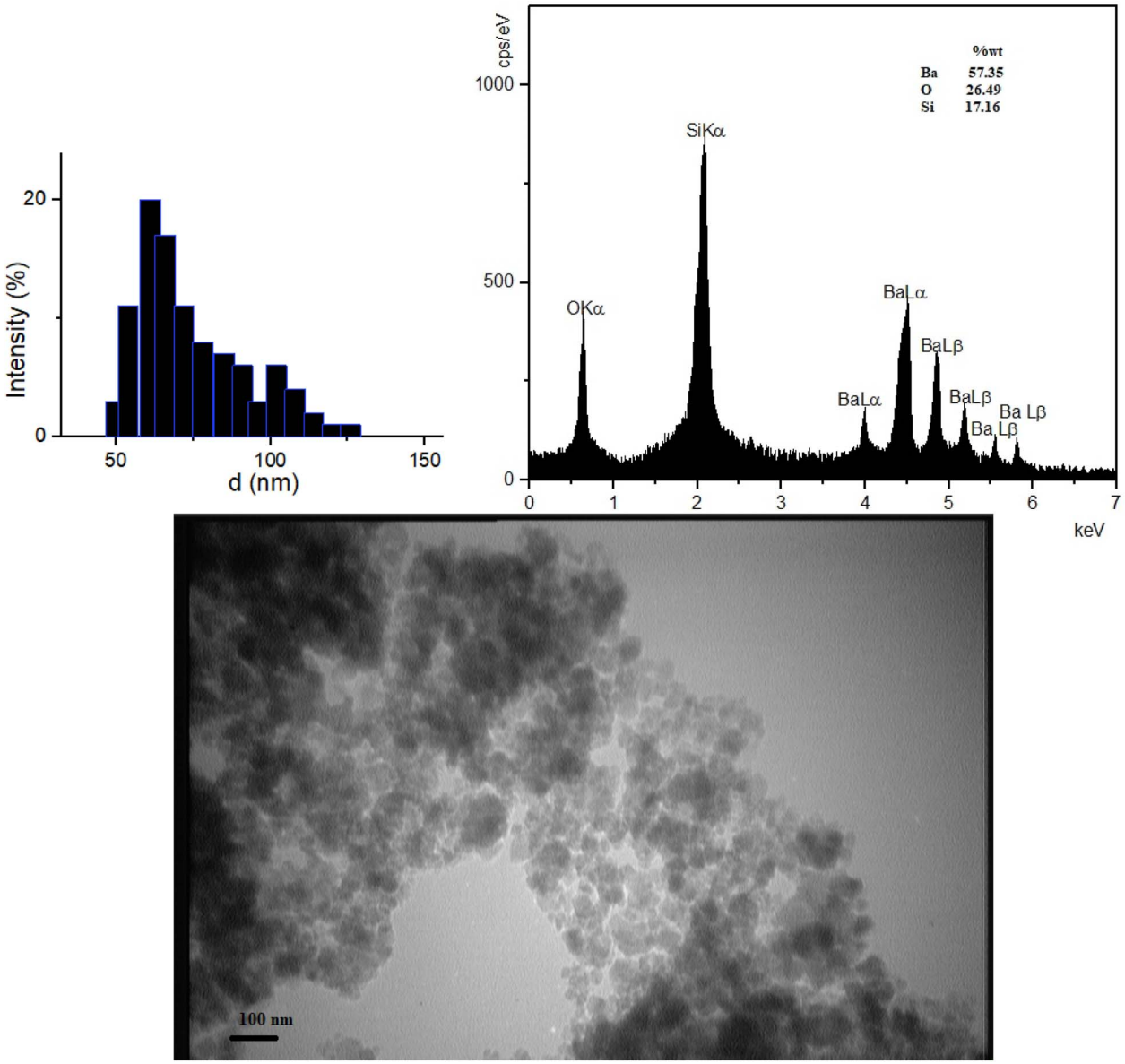

Fig. 2 DLS, EDS analyses, and TEM photographs of $BaSiO_3$ nanoparticles.

recyclability of the catalyst and its good stability. The FT-IR spectrum (Fig. 3) of the recovered catalyst confirms the structural stability of the compound.

Therefore, based on the purpose of this study, efficacy, generality, and the use of barium silicate as an efficient catalyst for the preparation of various α-benzyl amino coumarin derivatives was investigated by using different aromatic aldehydes containing electron-donating or electron-withdrawing groups (Scheme 1). The results are summarized in Table 2.

2.2. *In silico* ADMET modeling studies

The ADME properties have a significant role in the acceptance or rejection of compounds as potential drug candidates. In addition, toxicity is another property that can damage the organism. Hence, the study of ADMET properties of synthesized compounds before biological evaluation is necessary. The Swiss ADME software was utilized to predict the physiochemical properties of the synthesized compounds (**1–24**) according to Lipinski and Veber's rules. The molecular weights (MW) of all compounds were in the acceptable range (321–416 g mol^{-1}). The hydrogen bond properties (as donors or acceptors), total polar surface area (TPSA), and the rotatable bond number value of all synthesized compounds were reasonable. Moreover, all of the compounds had admissible lipophilicity (logP) values. Based on these physiochemical properties, all of the α-benzyl amino coumarin derivatives represented good potential for oral bioavailability (Table 3).

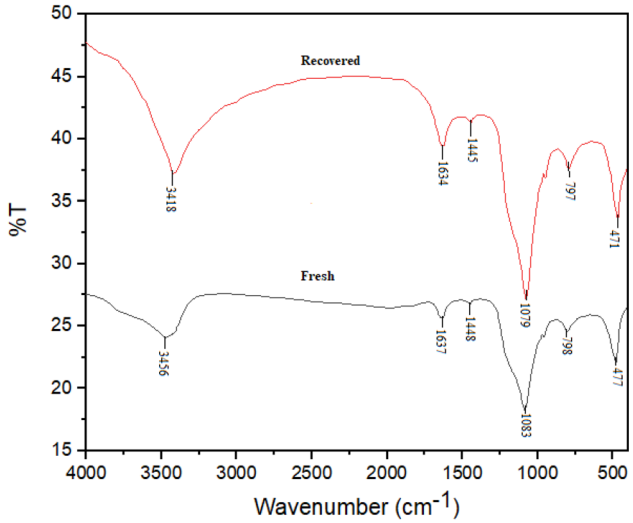

Fig. 3 FT-IR analysis of $BaSiO_3$ nanoparticles.

Table 1 Optimization of the reaction conditions in the synthesis of 4-hydroxy-3-(phenyl(piperidine-1-yl)methyl)-2*H*-chromium-2-one[a]

Entry	Catalyst (mmol)	*T* (°C)	Solvent (5 ml)	Yield[b] (%)
1	0.56	r.t.	—	10
2	0.56	r.t.	*n*-Hexane	—
3	0.56	r.t.	CH_2Cl_2	—
4	0.56	r.t.	Et_2O	—
5	0.56	r.t.	EtOAc	—
6	0.56	r.t.	EtOH	10
7	0.56	r.t.	MeOH	40
8	0.56	r.t.	H_2O	79
9	0.14	r.t.	H_2O	51
10	0.28	r.t.	H_2O	85
11	1	r.t.	H_2O	85

[a] Time for reaction: 2 hours. [b] Isolated yield.

The absorption and distribution properties of the synthesized compounds are displayed in Table 4. The log *S* value shows the water solubility, which is in the range of −3.63 to −2.18 for all tested compounds. In fact, their lower log *S* values represented better solubility. The human intestinal absorptions (% HIA) were above 95, which indicated high intestinal absorption in the transport of oral drugs to their biological targets. The Caco-2 permeability of all compounds except analogue **21**, illustrated that they exhibit permeability across intestinal membranes. In the case of blood–brain barrier property, compounds **6**, **8**, **14**, **16–17**, and **19–22** showed low blood–brain barrier percentages, respectively, leading to a lower neurological effect. Table 4 indicates that all of the tested compounds had no effects on P-glycoprotein efflux transporters as both substrate and inhibitor, therefore, these systems do not disturb the cell permeability and absorption of the compounds. The binding of drug molecules to plasma proteins can affect their bioavailability and distribution across cell membranes. Thus, the percentages of plasma protein binding (PPB) of all compounds was also calculated. All of them had weak PPB with values lower than 90%, except for **3**,**9**, **12**, and **19** which showed strong binding to plasma proteins.[26]

Table 5, illustrates the metabolism and toxicity profiles of all synthesized compounds. Both CYP2D6 and CYP3A4 enzymes have a crucial role in the metabolism of drugs in the liver. In this regard, compounds **1–10** and **21–24** were neither substrates nor inhibitors of CYP2D6 while compounds **11–20** were both substrates and inhibitors of CYP2D6. In the case of CYP3A4 enzymes, none of the compounds were substrates/inhibitors of CYP3A4, except for **14**, **16**, and **22**. The Ames test results represented that compounds **2–3**, **6–7**, **9–10**, **12–13**, **19–20**, and **23–24** had negative values which indicated their non-mutagenic behavior. All the tested compounds were determined to be non-carcinogenic and, showed lower oral toxicity, so could be considered safe through oral

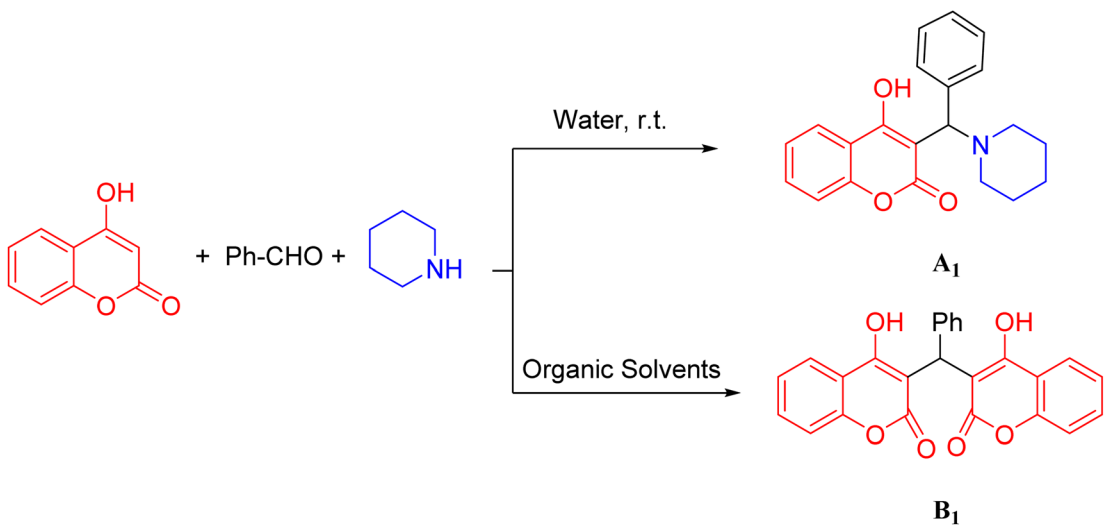

Scheme 2 Multi-component reaction of benzaldehyde, piperidine, and 4-hydroxycomarin in water and organic solvents.

Table 2 Synthesis of α-benzyl amino coumarin derivatives using barium silicate nanoparticles

Entry	Aldehyde	Amine	Product	Time (min)	Yield[a] (%)
1	Benzaldehyde	Piperidine	A_1	30	85
2	2-Chlorobenzaldehyde	Piperidine	A_2	60	87
3	4-Chlorobenzaldehyde	Piperidine	A_3	40	70
4	2-Methylbenzaldehyde	Piperidine	A_4	70	84
5	4-Methylbenzaldehyde	Piperidine	A_5	60	81
6	4-Methoxybenzaldehyde	Piperidine	A_6	70	70
7	4-*tert*-Butylbenzaldehyde	Piperidine	A_7	40	89
8	3-Nitrobenzaldehyde	Piperidine	A_8	25	90
9	2,4-Dichlorobenzaldehyde	Piperidine	A_9	75	61
10	4-Bromobenzaldehyde	Piperidine	A_{10}	40	90
11	Benzaldehyde	Pyrrolidine	A_{11}	45	82
12	4-Bromobenzaldehyde	Pyrrolidine	A_{12}	30	90
13	4-Chlorobenzaldehyde	Pyrrolidine	A_{13}	30	93
14	4-Nitrobenzaldehyde	Pyrrolidine	A_{14}	25	88
15	4-Methylbenzaldehyde	Pyrrolidine	A_{15}	65	89
16	4-Methoxybenzaldehyde	Pyrrolidine	A_{16}	80	95
17	3-Nitrobenzaldehyde	Pyrrolidine	A_{17}	30	92
18	Benzaldehyde	Morpholine	A_{18}	45	93
19	4-Bromobenzaldehyde	Morpholine	A_{19}	40	90
20	4-Chlorobenzaldehyde	Morpholine	A_{20}	35	98
21	4-Nitrobenzaldehyde	Morpholine	A_{21}	30	78
22	4-Methylbenzaldehyde	Morpholine	A_{22}	55	90
23	2,4-Dichlorobenzaldehyde	Morpholine	A_{23}	45	92
24	3,5-Dchlorobenzaldehyde	Morpholine	A_{24}	30	89
25	Butyraldehyde	Piperidine	A_{25}	120	—
26	Butyraldehyde	Pyrrolidine	A_{26}	120	—
27	Butyraldehyde	Morpholine	A_{27}	120	—
28	Hexanal	Piperidine	A_{28}	120	—
29	Hexanal	Pyrrolidine	A_{29}	120	—
30	Hexanal	Morpholine	A_{30}	120	—

[a] Isolated yield.

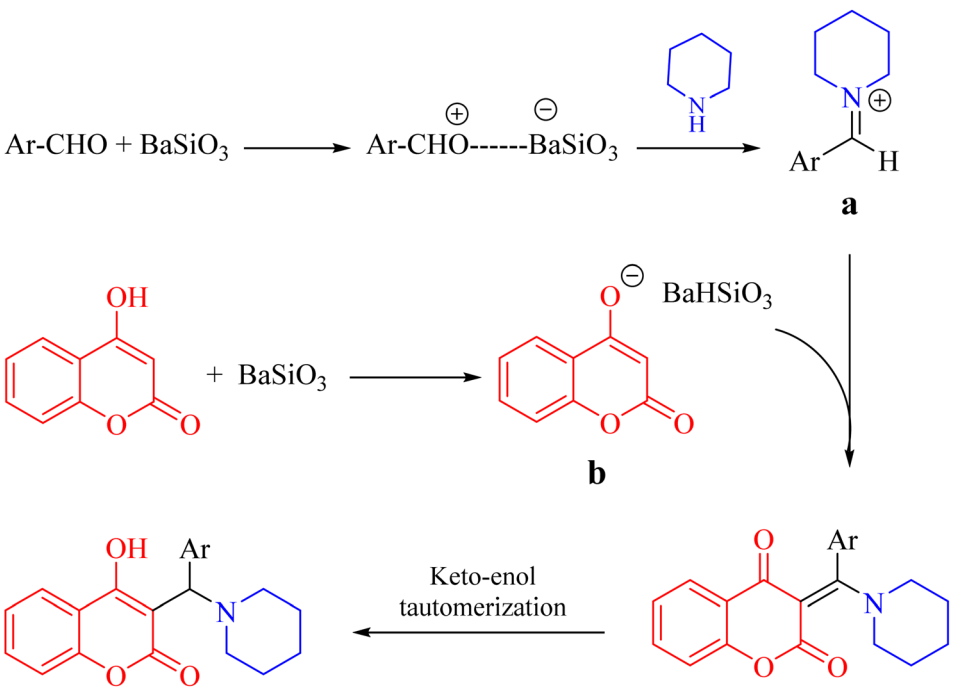

Scheme 3 Proposed mechanism of the reaction for the synthesis of α-benzyl amino coumarin derivatives.

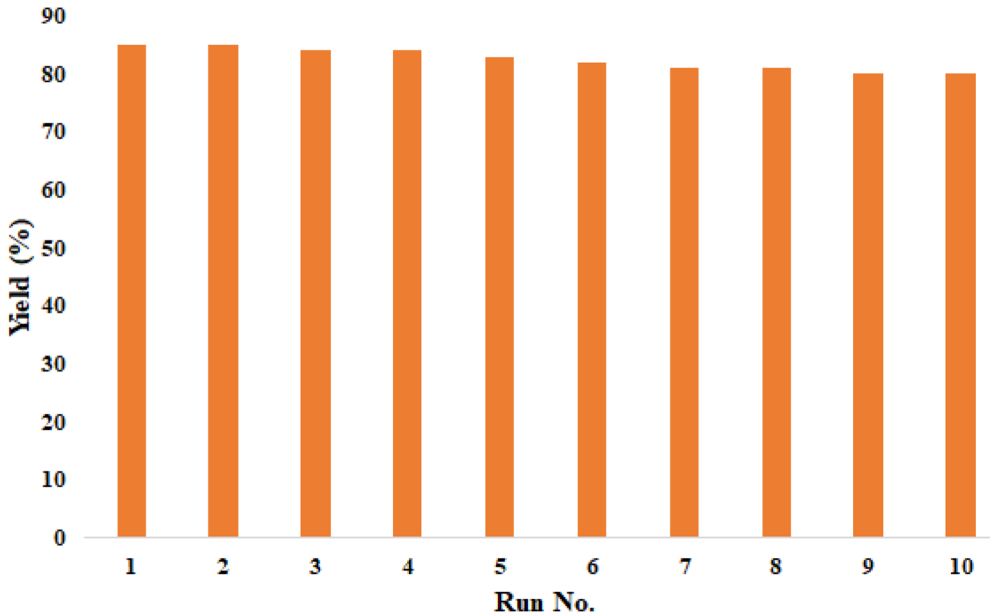

Fig. 4 The recyclability test results of $BaSiO_3$.

Table 3 Physiochemical properties of all α-benzyl amino coumarin derivatives (1–24)

Entry	MW[a]	LogP[b]	HBD[c]	HBA[d]	TPSA[e] (Å)	RB[f]	Lipinski/Veber violation
1	335.4	3.04	1	4	53.68	3	0
2	369.84	3.62	1	4	53.68	3	0
3	369.84	3.52	1	4	53.68	3	0
4	349.42	3.26	1	4	53.68	3	0
5	349.42	3.26	1	4	53.68	3	0
6	365.42	2.69	1	5	62.91	4	0
7	391.50	3.89	1	4	53.68	4	0
8	380.39	2.08	1	6	99.5	4	0
9	404.29	4.01	1	4	53.68	3	0
10	414.29	3.63	1	4	53.68	3	0
11	321.37	2.381	1	4	53.68	3	0
12	400.27	3.41	1	4	53.68	3	0
13	355.81	3.30	1	4	53.68	3	0
14	366.37	1.85	1	6	99.50	4	0
15	335.40	3.04	1	4	53.68	3	0
16	351.40	2.48	1	5	62.91	4	0
17	366.67	1.85	1	6	99.50	4	0
18	337.37	1.93	1	5	62.91	3	0
19	416.27	2.59	1	5	62.91	3	0
20	371.81	2.48	1	5	62.91	3	0
21	382.37	1.06	1	7	108.73	4	0
22	351.40	2.21	1	5	62.91	3	0
23	406.26	2.96	1	5	62.91	3	0
24	402.26	2.96	1	5	62.91	3	0
Lipinski/Veber's rules	≤ 500	≤ 5	≤ 5	≤ 10	≤ 140	≤ 10	≤ 1

[a] Molecular weight (MW). [b] Logarithm of partition coefficient between *n*-octanol and water (logP). [c] Number of hydrogen bond donors (HBD). [d] Number of hydrogen bond acceptors (HBA). [e] Topological polar surface area (TPSA). [f] Number of rotatable bonds (RB).

administration. Most of the compounds have weak hERG inhibition, which means that they could not affect QT interval prolongation and cause violent cardiac side effects. Taken together, these results indicate that these synthesized compounds had proper physicochemical and pharmacokinetic properties which would introduce them as ideal candidates for further biological evaluations.

Table 4 Absorption and distribution profile of all α-benzyl amino coumarin compounds[a]

Entry	HIA	Caco-2 permeability	BBB	P-Glycoprotein	Plasma protein bonding (PPB)
1	95.89	40.71	0.53	NS/NI	84.19
2	96.35	32.78	1.36	NS/NI	88.44
3	96.35	33.20	1.45	NS/NI	95.61
4	95.99	42.25	1.07	NS/NI	84.00
5	95.99	41.68	1.27	NS/NI	84.18
6	95.94	43.59	0.18	NS/NI	83.07
7	96.28	46.85	3.17	NS/NI	86.23
8	96.85	21.52	0.01	NS/NI	88.55
9	96.73	36.52	3.21	NS/NI	98.25
10	96.04	44.79	1.02	NS/NI	85.61
11	95.79	36.93	0.89	NS/NI	78.15
12	96.55	29.35	0.82	NS/NI	100
13	96.26	30.41	0.72	NS/NI	89.90
14	96.50	16.70	0.01	NS/NI	82.31
15	95.89	38.05	0.60	NS/NI	80.51
16	95.87	40.30	0.10	NS/NI	78.83
17	96.50	21.34	0.01	NS/NI	83.07
18	95.83	37.64	0.60	NS/NI	51.66
19	96.46	29.18	0.15	NS/NI	91.28
20	96.16	30.91	0.14	NS/NI	78.08
21	95.23	9.96	0.01	NS/NI	66.81
22	95.88	38.05	0.07	NS/NI	60.53
23	96.59	33.57	0.27	NS/NI	86.02
24	96.59	33.64	0.50	NS/NI	88.18

[a] NS = non-substrate; NI = non-inhibitor; S = substrate; I = inhibitor.

Table 5 Metabolism and toxicity profile of all α-benzyl amino coumarin compounds[a]

Entry	CYP2D6	CYP3A4	AMES toxicity	Carcinogenicity	hERG inhibition
1	NS/NI	NS/NI	Toxic	NC	Weak
2	NS/NI	NS/NI	Non toxic	NC	Strong
3	NS/NI	NS/NI	Non toxic	NC	Strong
4	NS/NI	NS/NI	Toxic	NC	Weak
5	NS/NI	NS/NI	Toxic	NC	Weak
6	NS/NI	NS/NI	Non toxic	NC	Weak
7	NS/NI	NS/NI	Non toxic	NC	Weak
8	NS/NI	NS/NI	Toxic	NC	Strong
9	NS/NI	NS/NI	Non toxic	NC	Strong
10	NS/NI	NS/NI	Non toxic	NC	Weak
11	S/I	NS/NI	Toxic	NC	Weak
12	S/I	NS/NI	Non toxic	NC	Weak
13	S/I	NS/NI	Non toxic	NC	Weak
14	S/I	S/I	Toxic	NC	Weak
15	S/I	NS/NI	Toxic	NC	Weak
16	S/I	S/NI	Toxic	NC	Weak
17	S/I	NS/NI	Toxic	NC	Weak
18	S/I	NS/NI	Toxic	NC	Weak
19	S/I	NS/NI	Non toxic	NC	Weak
20	S/I	NS/NI	Non toxic	NC	Weak
21	NS/NI	NS/NI	Toxic	NC	Weak
22	NS/NI	S/I	Toxic	NC	Weak
23	NS/NI	NS/NI	Non toxic	NC	Weak
24	NSN/I	NS/NI	Non toxic	NC	Weak

[a] hERG = Human ether-a-go-go related gene, NS = non-substrate; NI = non-inhibitor; S = substrate; I = inhibitor; NC = non-carcinogenic; C = carcinogenic.

3. Experimental

3.1. Reagents and instrumentation

All reagents were purchased from Merck and Aldrich and used without further purification. All yields refer to isolated products after purification. The NMR spectra were recorded on a Bruker Advance DPX 400 MHz instrument. The spectra were measured in DMSO-d6 relative to TMS (0.00 ppm). Elemental analysis was performed on a Heraeus CHN-O-Rapid analyser. TLC was performed on silica gel PolyGram SIL G/UV 254 plates. The powder X-ray diffraction patterns were measured with D8, Advance, Bruker, AXS, and diffractometer using CuKα irradiation. FE-SEM was taken by a Hitachi S-4160 photograph to examine the shape and size of $BaSiO_3$ nanoparticles.

3.2. Preparation of barium silicate nanopowder

10 ml $BaCl_2$ and 10 ml tetra ethyl orthosilicate were dissolved in 150 ml ethanol. Then ammonium 18% was added dropwise, while vigorously stirring at room temperature for 24 h. The resultant mixture was aged for 10 h. The gel was dried at 100 °C for 3 h and calcination at 1000 °C for 3 h. The resulting barium silicate was pulverized.[25]

3.3. General procedure

To a mixture of aldehyde (1.2 mmol), piperidine or other aliphatic amines (1.2 mmol) and 4-hydroxycoumarin (1 mmol) in water (5 ml), $BaSiO_3$ nanopowder (0.26 mmol) as a catalyst was added and the mixture was stirred for a period of time at room temperature (Table 2). Progress of the reaction was monitored by TLC using *n*-hexane/ethyl acetate (9 : 1). Upon completion, the solvent was evaporated and the reaction mixture was diluted in hot ethanol. The catalyst was isolated by simple filtration, and the crude product was recrystallized in ethanol/water (75 : 25) to afford the pure product.

3.4. Spectral data

3.4.1. 4-Hydroxy-3-(phenyl(piperidin-1-yl) methyl)-2*H*-chromen-2-one (A1). Yield: 85% (0.285 mg), white solid, m.p.: 183–185 °C; ^{1}H-NMR (400 MHz, DMSO-d_6): δ = 1.81–1.91 (m, 6H), 2.24–2.31 (m, 2H), 3.05–3.12 (m, 2H), 5.36 (s, 1H), 7.19 (t, J = 7.6 Hz, 2H), 7.27 (t, J = 7.6 Hz, 1H), 7.34 (d, J = 7.6 Hz, 2H), 7.43 (t, J = 8.2 Hz, 1H), 7.52 (d, J = 8.2 Hz, 1H), 7.80 (t, J = 8.2 Hz, 1H), 7.89 (d, J = 8.4 Hz, 1H), 8.00–8.11 (brs, 1H, OH) ppm; ^{13}C-NMR (100 MHz, DMSO-d_6): δ = 22.1, 24.8, 49.6, 71.6, 103.3, 115.3, 119.5, 122.6, 125.3, 127.4, 128.7, 129.7, 130.3, 135.2, 154.5, 162.9, 174.2 ppm; elemental analysis for $C_{21}H_{21}NO_3$: found: C, 75.12; H, 6.24; N, 4.14%; calculated: C, 75.20; H, 6.31; N, 4.18%.

3.4.2. 3-((2-Chlorophenyl)(piperidin-1-yl)methyl)-4-hydroxy-2*H*-chromen-2-one (A2). Yield: 87% (0.322 mg), white solid, m.p.: 186–188 °C; ^{1}H-NMR (400 MHz, DMSO-d_6): δ = 1.80–1.92 (m, 6H), 2.24–2.31 (m, 2H), 3.04–3.12 (m, 2H), 5.48 (s, 1H), 7.22 (t, J = 7.6 Hz, 1H), 7.28 (t, J = 7.8 Hz, 1H), 7.37 (d, J = 7.8 Hz, 1H), 7.44 (t, J = 8.0 Hz, 1H), 7.53 (d, J = 8.0 Hz, 1H), 7.64 (d, J = 7.7 Hz, 1H), 7.79–7.85 (m, 2H), 7.90 (d, J = 8.4 Hz, 1H) ppm; ^{13}C-NMR (100 MHz, DMSO-d_6): δ = 22.4, 25.0, 50.41, 74.7, 105.0, 116.1, 120.3, 125.0, 128.6, 129.1, 129.6, 130.1, 130.7, 131.3, 136.1, 144.2, 155.2, 164.4, 174.6 ppm; elemental analysis for $C_{21}H_{20}ClNO_3$: found: C, 68.26; H, 5.52; N, 3.73%; calculated: C, 68.20; H, 5.45; N, 3.79%.

3.4.3. 3-((4-Chlorophenyl)(piperidin-1-yl)methyl)-4-hydroxy-2*H*-chromen-2-one (A3). Yield: 70% (0.259 mg), white solid, m.p.: 189–191 °C; ^{1}H-NMR (400 MHz, DMSO-d_6): δ = 1.82–1.91 (m, 6H), 2.21–2.30 (m, 2H), 3.06–3.12 (m, 2H), 5.48 (s, 1H), 7.24 (d, J = 7.7 Hz, 2H), 7.42–7.54 (m, 5H), 7.81 (t, J = 8.2 Hz, 1H), 7.90 (d, J = 8.4 Hz, 1H), ppm; ^{13}C-NMR (100 MHz, DMSO-d_6): δ = 21.4, 25.1, 49.7, 73.5, 104.5, 115.4, 120.7, 124.2, 129.3, 130.1, 130.7, 132.8, 135.2, 145.1, 154.7, 164.5, 174.3 ppm; elemental analysis for $C_{21}H_{20}ClNO_3$: found: C, 68.14; H, 5.53; N, 3.87%; calculated: C, 68.20; H, 5.45; N, 3.79%.

3.4.4. 4-Hydroxy-3-(piperidin-1-yl(*o*-tolyl) methyl)-2*H*-chromen-2-one (A4). Yield: 84% (0.293 mg), white solid, m.p.: 201–203 °C; ^{1}H-NMR (400 MHz, DMSO-d_6): δ = 1.82–1.93 (m, 6H), 2.24–2.30 (m, 2H), 3.07–3.12 (m, 2H), 5.31 (s, 1H), 7.06 (d, J = 7.8 Hz, 1H), 7.12 (t, J = 7.8 Hz, 1H), 7.25–7.30 (m, 2H), 7.42 (t, J = 8.2 Hz, 1H), 7.52 (d, J = 8.0 Hz, 1H), 7.79 (t, J = 8.1 Hz, 1H), 7.88 (d, J = 8.2 Hz, 1H), 8.10–8.40 (m, 1H, OH) ppm; ^{13}C-NMR (100 MHz, DMSO-d_6): δ = 21.1, 21.7, 25.4, 49.6, 73.7, 103.8, 115.1, 120.2, 123.9, 124.5, 126.8, 127.4, 127.8, 130.4, 131.0, 134.0, 137.2, 154.8, 163.9, 173.7 ppm; elemental analysis for $C_{22}H_{23}NO_3$: found: C, 75.54; H, 6.58; N, 4.11%; calculated: C, 75.62; H, 6.63; N, 4.01%.

3.4.5. 4-Hydroxy-3-(piperidin-1-yl(*p*-tolyl) methyl)-2*H*-chromen-2-one (A5). Yield: 81% (0.282 mg), white solid, m.p.: 197–199 °C; ^{1}H-NMR (400 MHz, DMSO-d_6): δ = 1.78–1.89 (m, 6H), 2.20–2.27 (m, 2H), 2.31 (s, 3H), 3.06–3.13 (m, 2H), 5.14 (s, 1H), 7.24 (d, J = 7.7 Hz, 2H), 7.42–7.54 (m, 5H), 7.81 (t, J = 8.2 Hz, 1H), 7.90 (d, J = 8.4 Hz, 1H), 7.13 (d, J = 7.7 Hz, 2H), 7.24 (d, J = 7.7 Hz, 2H), 7.42 (t, J = 8.4 Hz, 1H), 7.51 (d, J = 8.4 Hz, 1H), 7.79 (t, J = 8.2 Hz, 1H), 7.88 (d, J = 8.2 Hz, 1H) ppm; ^{13}C-NMR (100 MHz, DMSO-d_6): δ = 21.5, 22.4, 25.6, 49.9, 73.5, 103.9, 115.4, 120.1, 121.8, 124.5, 127.8, 130.4, 131.0, 134.0, 137.7, 154.7, 163.6, 173.9 ppm; elemental analysis for $C_{22}H_{23}NO_3$: found: C, 75.66; H, 6.72; N, 4.08%; calculated: C, 75.62; H, 6.63; N, 4.01%.

3.4.6. 4-Hydroxy-3-((4-methoxyphenyl)(piperidin-1-yl) methyl)-2*H*-chromen-2-one (A6). Yield: 70% (0.256 mg), white solid, m.p.: 192–194 °C; ^{1}H-NMR (400 MHz, DMSO-d_6): δ = 1.79–1.86 (m, 6H), 2.22–2.27 (m, 2H), 3.08–3.11 (m, 2H), 3.79 (s, 3H), 4.09 (s, 1H), 6.96 (d, J = 7.7 Hz, 2H), 7.12 (d, J = 7.7 Hz, 2H), 7.42 (t, J = 8.4 Hz, 1H), 7.51 (d, J = 8.4 Hz, 1H), 7.79 (t, J = 8.2 Hz, 1H), 7.88 (d, J = 8.2 Hz, 1H) ppm; ^{13}C-NMR (100 MHz, DMSO-d_6): δ = 21.6, 25.5, 50.1, 56.1, 73.4, 103.7, 115.6, 117.2, 121.6, 124.1, 124.2, 129.1, 130.1, 131.0, 154.6, 156.2, 163.4, 173.1 ppm; elemental analysis for $C_{22}H_{23}NO_4$: found: C, C, 72.37; H, 6.39; N, 3.89%; calculated: C, 72.31; H, 6.34; N, 3.83%.

3.4.7. 3-((4-(*tert*-Butyl)phenyl)(piperidin-1-yl)methyl)-4-hydroxy-2*H*-chromen-2-one (A7). Yield: 89% (0.348 mg), white solid, m.p.: 207–209 °C; ^{1}H-NMR (400 MHz, DMSO-d_6): δ = 1.29 (s, 9H), 1.82–1.89 (m, 6H), 2.23–2.26 (m, 2H), 3.04–3.09 (m, 2H), 5.29 (s, 1H), 7.14 (d, J = 7.7 Hz, 2H), 7.25 (d, J = 7.7 Hz, 2H), 7.43 (t, J = 8.4 Hz, 1H), 7.52 (d, J = 8.4 Hz, 1H), 7.80 (t, J = 8.2 Hz, 1H),

7.89 (d, J = 8.2 Hz, 1H), ppm; ^{13}C-NMR (100 MHz, DMSO-d_6): δ = 14.8, 21.4, 25.5, 34.3, 50.3, 73.6, 103.4, 115.4, 121.6, 124.7, 126.7, 127.9, 130.2, 131.2, 133.5, 138.2, 154.5, 163.1, 173.5 ppm; elemental analysis for $C_{25}H_{29}NO_3$: found: C, 76.77; H, 7.53; N, 3.51%; calculated: C, 76.70; H, 7.47; N, 3.58%.

3.4.8. 4-Hydroxy-3-((3-nitrophenyl)(piperidin-1-yl) methyl)-2*H*-chromen-2-one (A_8). Yield: 90% (0.342 mg), yellow solid, m.p.: 218–220 °C; ^{1}H-NMR (400 MHz, DMSO-d_6): δ = 1.83–1.92 (m, 6H), 2.25–2.29 (m, 2H), 3.08–3.13 (m, 2H), 5.72 (s, 1H), 7.44 (t, J = 8.0 Hz, 1H), 7.51 (d, J = 8.0 Hz, 1H), 7.56 (t, J = 7.8 Hz, 1H), 7.80 (t, J = 8.0 Hz, 1H), 7.91 (d, J = 8.1 Hz, 1H), 8.27 (d, J = 7.8 Hz, 1H), 8.02 (d, J = 7.8 Hz, 1H), 8.49 (s, 1H), 8.50–8.90 (m, 1H, OH) ppm; ^{13}C-NMR (100 MHz, DMSO-d_6): δ = 21.9, 25.7, 50.5, 75.6, 103.7, 115.9, 121.7, 124.8, 128.7, 129.1, 129.6, 130.1, 130.9, 131.4, 134.5, 139.2, 154.7, 164.1, 175.5 ppm; elemental analysis for $C_{21}H_{20}N_2O_5$: found: C, 66.26; H, 5.25; N, 7.31%; calculated: C, 66.31; H, 5.30; N, 7.36%.

3.4.9. 3-((2,4-Dichlorophenyl)(piperidin-1-yl)methyl)-4-hydroxy-2*H*-chromen-2-one (A_9). Yield: 61% (0.246 mg), white solid, m.p.: 211–213 °C; ^{1}H-NMR (400 MHz, DMSO-d_6): δ = 1.84–1.90 (m, 6H), 2.25–2.28 (m, 2H), 3.08–3.12 (m, 2H), 5.52 (s, 1H), 7.41–7.51 (m, 3H), 7.69 (d, J = 7.8 Hz, 1H), 7.77–7.81 (m, 2H), 7.88 (d, J = 8.3 Hz, 1H) 7.95–8.30 (m, 1H, OH) ppm; ^{13}C-NMR (100 MHz, DMSO-d_6): δ = 21.7, 25.8, 50.3, 74.3, 103.5, 115.7, 122.0, 124.6, 127.7, 128.9, 129.3, 130.2, 131.4, 134.1, 141.2, 143.6, 154.6, 163.9, 174.5 ppm; elemental analysis for $C_{21}H_{19}Cl_2NO_3$: found: C, 62.39; H, 4.74; N, 3.46%; calculated: C, 62.39; H, 4.74; N, 3.46%.

3.4.10. 3-((4-Bromophenyl)(piperidin-1-yl)methyl)-4-hydroxy-2*H*-chromen-2-one (A_{10}). Yield: 90% (0.373 mg), white solid, m.p.: 203–205 °C; ^{1}H-NMR (400 MHz, DMSO-d_6): δ = 1.78–1.88 (m, 6H), 2.22–2.28 (m, 2H), 3.08–3.14 (m, 2H), 5.59 (s, 1H), 7.39–7.52 (m, 5H), 7.75–7.89 (m, 5H) ppm; ^{13}C-NMR (100 MHz, DMSO-d_6): δ = 21.7, 25.4, 49.8, 73.9, 103.5, 115.1, 121.6, 124.3, 128.9, 130.2, 131.3, 132.9, 133.7, 148.3, 154.7, 163.9, 174.7 ppm; elemental analysis for $C_{21}H_{20}BrNO_3$: found: C, 60.85; H, 4.82; N, 3.31%; calculated: C, 60.88; H, 4.87; N, 3.38%.

3.4.11. 4-Hydroxy-3-(phenyl(pyrrolidin-1-yl) methyl)-2*H*-chromen-2-one (A11). Yield: 82% (0.264 mg), white solid, m.p.: 167–169 °C; ^{1}H-NMR (400 MHz, DMSO-d_6): δ = 2.02–2.10 (m, 4H), 3.02–3.08 (m, 2H), 3.41–3.47 (m, 2H), 5.19 (s, 1H), 7.19–7.33 (m, 5H), 7.41 (t, J = 8.4 Hz, 1H), 7.49 (d, J = 8.2 Hz, 1H), 7.69 (t, J = 8.3 Hz, 1H), 7.93 (d, J = 8.2 Hz, 1H), 7.99 (brs, 1H, OH) ppm; ^{13}C-NMR (100 MHz, DMSO-d_6): δ = 26.7, 53.6, 72.3, 103.5, 115.7, 120.1, 123.6, 125.7, 127.8, 128.6, 129.5, 130.3, 134.9, 154.7, 163.1, 173.9 ppm; elemental analysis for $C_{20}H_{19}NO_3$: found: C, 74.69; H, 5.99; N, 4.42; calculated: C, 74.75; H, 5.96; N, 4.36%.

3.4.12. 3-((4-Bromophenyl) (pyrrolidin-1-yl)methyl)-4-hydroxy-2*H*-chromen-2-one (A12). Yield: 90% (0.360 mg), white solid, m.p.: 188–190 °C; ^{1}H-NMR (400 MHz, DMSO-d_6): δ = 2.04–2.11 (m, 4H), 3.01–3.06 (m, 2H), 3.41–3.43 (m, 2H), 5.39 (s, 1H), 7.35 (d, J = 7.7 Hz, 2H), 7.40 (t, J = 8.4 Hz, 1H), 7.48 (d, J = 8.2 Hz, 1H), 7.65 (d, J = 7.7 Hz, 2H), 7.67 (t, J = 8.3 Hz, 1H), 7.90 (d, J = 8.2 Hz, 1H), 7.96 (brs, 1H, OH) ppm; ^{13}C-NMR (100 MHz, DMSO-d_6): δ = 26.4, 53.6, 74.2, 103.7, 115.1, 121.6, 124.5, 128.8, 130.2, 131.2, 133.3, 134.6, 148.1, 154.7, 164.1, 174.8 ppm; elemental analysis for $C_{20}H_{18}BrNO_3$: found: C, 60.08; H, 4.59; N, 3.55; calculated: C, 60.01; H, 4.53; N, 3.50%.

3.4.13. 3-((4-Chlorophenyl) (pyrrolidin-1-yl)methyl)-4-hydroxy-2*H*-chromen-2-one (A13). Yield: 93% (0.331 mg), white solid, m.p.: 175–177 °C; ^{1}H-NMR (400 MHz, DMSO-d_6): δ = 2.04–2.12 (m, 4H), 3.00–3.06 (m, 2H), 3.40–3.46 (m, 2H), 5.46 (s, 1H), 7.27 (d, J = 7.7 Hz, 2H), 7.41 (t, J = 8.4 Hz, 1H), 7.48 (d, J = 7.7 Hz, 2H), 7.52 (d, J = 8.4 Hz, 1H), 7.67 (brs, 1H, OH), 7.80 (t, J = 8.2 Hz, 1H), 7.90 (d, J = 8.2 Hz, 1H) ppm; ^{13}C-NMR (100 MHz, DMSO-d_6): δ = 26.4, 52.8, 74.1, 105.9, 115.8, 121.2, 124.6, 129.8, 130.1, 131.3, 132.8, 135.1, 144.5, 154.7, 164.1, 174.8 ppm; elemental analysis for $C_{20}H_{18}ClNO_3$: found: C, 67.44; H, 5.02; N, 3.85; calculated: C, 67.51; H, 5.10; N, 3.94%.

3.4.14. 4-Hydroxy-3-((4-nitrophenyl) (pyrrolidin-1-yl) methyl)-2*H*-chromen-2-one (A14). Yield: 88% (0.322 mg), yellow solid, m.p.: 193–195 °C; ^{1}H-NMR (400 MHz, DMSO-d_6): δ = 2.06–2.12 (m, 4H), 3.04–3.07 (m, 2H), 3.44–3.47 (m, 2H), 5.76 (s, 1H), 7.42 (t, J = 8.3 Hz, 1H), 7.52 (d, J = 8.3 Hz, 1H), 7.77 (d, J = 7.9 Hz, 2H), 7.81 (t, J = 8.3 Hz, 1H), 7.91 (d, J = 8.3 Hz, 1H), 7.90–8.20 (brs, 1H, OH), 8.28 (d, J = 7.8 Hz, 2H) ppm; ^{13}C-NMR (100 MHz, DMSO-d_6): δ = 26.4, 53.4, 77.4, 106.1, 116.0, 121.2, 124.6, 130.2, 130.6, 131.4, 134.1, 137.1, 139.5, 154.8, 164.6, 175.6 ppm; elemental analysis for $C_{20}H_{18}N_2O_5$: found: C, 65.66; H, 4.99; N, 7.61; calculated: C, 65.57; H, 4.95; N, 7.65%.

3.4.15. 4-Hydroxy-3-(pyrrolidin-1-yl(*p*-tolyl)methyl)-2*H*-chromen-2-one (A15). Yield: 89% (0.299 mg), white solid, m.p.: 176–178 °C; ^{1}H-NMR (400 MHz, DMSO-d_6): δ = 2.01–2.09 (m, 4H), 2.28 (s, 3H), 3.01–3.05 (m, 2H), 3.41–3.45 (m, 2H), 5.16 (s, 1H), 7.01 (d, J = 7.7 Hz, 2H), 7.21 (d, J = 7.7 Hz, 2H), 7.40 (t, J = 8.4 Hz, 1H), 7.48 (d, J = 8.2 Hz, 1H), 7.69 (t, J = 8.3 Hz, 1H), 7.89–7.94 (m, 3H) ppm; ^{13}C-NMR (100 MHz, DMSO-d_6): δ = 21.6, 26.1, 51.2, 73.1, 104.8, 115.2, 120.1, 121.6, 124.7, 128.2, 130.2, 131.3, 134.1, 137.8, 154.5, 163.3, 173.2 ppm; elemental analysis for $C_{21}H_{21}NO_3$: found: C, 75.14; H, 6.27; N, 4.13; calculated: C, 75.20; H, 6.31; N, 4.18%.

3.4.16. 4-Hydroxy-3-((4-methoxyphenyl) (pyrrolidin-1-yl) methyl)-2*H*-chromen-2-one (A16). Yield: 95% (0.334 mg), white solid, m.p.: 174–176 °C; ^{1}H-NMR (400 MHz, DMSO-d_6): δ = 2.02–2.09 (m, 4H), 3.01–3.05 (m, 2H), 3.41–3.45 (m, 2H), 3.73 (s, 3H), 5.16 (s, 1H), 6.91 (d, J = 7.7 Hz, 2H), 7.07 (d, J = 7.7 Hz, 2H), 7.40 (t, J = 8.4 Hz, 1H), 7.48 (d, J = 8.2 Hz, 1H), 7.67–7.71 (m, 2H), 7.92 (d, J = 8.2 Hz, 1H) ppm; ^{13}C-NMR (100 MHz, DMSO-d_6): δ = 26.5, 51.1, 56.7, 73.1, 103.5, 115.8, 117.5, 121.4, 124.3, 124.8, 129.0, 130.3, 131.2, 154.6, 156.4, 163.6, 171.4 ppm; elemental analysis for $C_{21}H_{21}NO_4$: found: C, 71.74; H, 5.98; N, 3.95; calculated: C, 71.78; H, 6.02; N, 3.99%.

3.4.17. 4-Hydroxy-3-((3-nitrophenyl)(pyrrolidin-1-yl) methyl)-2*H*-chromen-2-one (A17). Yield: 92% (0.337 mg), yellow solid, m.p.: 195–197 °C; ^{1}H-NMR (400 MHz, DMSO-d_6): δ = 2.02–2.12 (m, 4H), 3.01–3.08 (m, 2H), 3.38–3.45 (m, 2H), 5.79 (s, 1H), 7.43 (t, J = 8.1 Hz, 1H), 7.52 (d, J = 8.1 Hz, 1H), 7.55 (t, J = 7.8 Hz, 1H), 7.78 (t, J = 8.2 Hz, 1H), 7.90 (d, J = 8.2 Hz, 1H), 7.98 (d, J = 7.8 Hz, 1H), 8.25 (d, J = 7.8 Hz, 1H), 8.47 (s, 1H), 9.40–9.70 (brs, 1H, OH) ppm; ^{13}C-NMR (100 MHz, DMSO-d_6): δ = 26.7, 51.8, 77.3, 104.1, 116.1, 121.5, 124.6, 128.9, 129.4, 129.9, 130.2, 131.2, 131.6, 135.3, 139.7, 154.6, 164.3, 176.4 ppm; elemental

analysis for $C_{20}H_{18}N_2O_5$: found: C, 65.64; H, 5.03; N, 7.63; calculated: C, 65.57; H, 4.95; N, 7.65%.

3.4.18. 4-Hydroxy-3-(morpholino(phenyl)methyl)-2*H*-chromen-2-one (A18). Yield: 93% (0.314 mg), white solid, m.p.: 172–174 °C; ^{1}H-NMR (400 MHz, DMSO-d$_6$): δ = 2.95–3.01 (m, 2H), 3.29–3.35 (m, 2H), 3.73–3.92 (m, 4H), 5.34 (s, 1H), 7.19–7.33 (m, 6H), 7.45 (t, J = 8.2 Hz, 1H), 7.55 (d, J = 8.3 Hz, 1H), 7.82 (t, J = 8.2 Hz, 1H), 7.90 (d, J = 8.2 Hz, 1H) ppm; ^{13}C-NMR (100 MHz, DMSO-d$_6$): δ = 59.8, 64.6, 74.6, 104.4, 116.2, 120.7, 123.6, 125.7, 127.6, 128.7, 129.6130.4, 136.4, 155.2, 163.9, 174.6 ppm; elemental analysis for $C_{20}H_{19}NO_4$: found: C, 71.26; H, 5.74; N, 4.08; calculated: C, 71.20; H, 5.68; N, 4.15%.

3.4.19. 3-((4-Bromophenyl)(morpholino)methyl)-4-hydroxy-2*H*-chromen-2-one (A19). Yield: 90% (0.375 mg), white solid, m.p.: 189–191 °C; ^{1}H-NMR (400 MHz, DMSO-d$_6$): δ = 2.96–3.02 (m, 2H), 3.31–3.95 (m, 6H), 5.44 (s, 1H), 7.32 (d, J = 7.7 Hz, 2H), 7.42–7.56 (m, 5H), 7.82 (t, J = 8.2 Hz, 1H), 7.91 (d, J = 8.2 Hz, 1H) ppm; ^{13}C-NMR (100 MHz, DMSO-d$_6$): δ = 60.4, 66.6, 78.2, 104.7, 116.1, 121.6, 124.4, 128.9, 130.2, 131.1, 133.4, 135.6, 148.4, 155.2, 164.3, 174.1 ppm; elemental analysis for $C_{20}H_{18}BrNO_4$: found: C, 57.75; H, 4.44; N, 3.42; calculated: C, 57.71; H, 4.36; N, 3.36%.

3.4.20. 3-((4-Chlorophenyl)(morpholino)methyl)-4-hydroxy-2*H*-chromen-2-one (A20). Yield: 98% (0.364 mg), white solid, m.p.: 171–173 °C; ^{1}H NMR (400 MHz, DMSO-d$_6$): δ = 2.94–3.97 (m, 8H), 5.67 (s, 1H), 7.26 (d, J = 7.8 Hz, 2H), 7.41–7.53 (m, 4H), 7.78 (t, J = 8.3 Hz, 1H), 7.90 (d, J = 8.3 Hz, 1H), 7.90–8.00 (brs, 1H, OH) ppm; ^{13}C-NMR (100 MHz, DMSO-d$_6$): δ = 60.1, 66.4, 76.7, 104.5, 116.0, 121.6, 124.3, 127.8, 129.6, 130.1, 131.3, 134.8, 142.4, 155.3, 164.1, 172.1 ppm; elemental analysis for $C_{20}H_{18}ClNO_4$: found: C, 64.53; H, 4.79; N, 3.81; calculated: C, 64.61; H, 4.88; N, 3.77%.

3.4.21. 4-Hydroxy-3-(morpholino(4-nitrophenyl) methyl)-2*H*-chromen-2-one (A21). Yield: 78% (0.298 mg), yellow solid, m.p.: 185–187 °C; ^{1}H-NMR (400 MHz, DMSO-d$_6$): δ = 2.96–3.94 (m, 8H), 6.39 (s, 1H), 7.42 (t, J = 8.4 Hz, 1H), 7.49 (d, J = 8.4 Hz, 1H), 7.67 (t, J = 8.4 Hz, 1H), 7.78 (d, J = 7.7 Hz, 2H), 7.94 (d, J = 8.4 Hz, 1H), 8.03 (d, J = 7.7 Hz, 2H), 7.90–8.00 (brs, 1H, OH) ppm; ^{13}C-NMR (100 MHz, DMSO-d$_6$): δ = 61.2, 68.3, 82.4, 106.3, 116.4, 121.3, 124.6, 129.3, 130.4, 131.3, 132.4, 137.3, 140.1, 155.2, 164.8, 178.9 ppm; elemental analysis for $C_{20}H_{18}N_2O_4$: found: C, 62.73; H, 4.71; N, 7.28%; calculated: C, 62.82; H, 4.75; N, 7.33%.

3.4.22. 4-Hydroxy-3-(morpholino(*p*-tolyl) methyl)-2*H*-chromen-2-one (A22). Yield: 90% (0.316 mg), white solid, m.p.: 173–175 °C; ^{1}H-NMR (400 MHz, DMSO-d$_6$): δ = 2.94–3.97 (m, 8H), 5.48 (s, 1H), 7.14 (d, J = 7.8 Hz, 2H), 7.26 (d, J = 7.8 Hz, 2H), 7.42 (t, J = 8.3 Hz, 1H), 7.51 (d, J = 8.3 Hz, 1H), 7.77 (t, J = 8.3 Hz, 1H), 7.89 (d, J = 8.3 Hz, 1H), 7.95–8.10 (brs, 1H, OH) ppm; ^{13}C-NMR (100 MHz, DMSO-d$_6$): δ = 21.5, 59.7, 65.8, 74.2, 104.9, 115.4, 120.2, 121.6, 124.7, 128.6, 130.1, 131.4, 134.0, 137.7, 154.5, 163.7, 174.2 ppm; elemental analysis for $C_{21}H_{21}NO_4$: found: C, 71.71; H, 6.09; N, 4.06%; calculated: C, 71.78; H, 6.02; N, 3.99%.

3.4.23. 3-((2,4-Dichlorophenyl)(morpholino)methyl)-4-hydroxy-2*H*-chromen-2-one (A23). Yield: 92% (0.374 mg), white solid, m.p.: 193–195 °C; ^{1}H-NMR (400 MHz, DMSO-d$_6$): δ = 2.95–3.99 (m, 8H), 5.82 (s, 1H), 7.41–7.46 (m, 3H), 7.50 (d, J = 8.3 Hz, 1H), 7.69 (d, J = 7.8 Hz, 1H), 7.79 (t, J = 8.2 Hz, 1H), 7.81 (s, 1H), 7.88 (d, J = 8.3 Hz, 1H), 7.94–8.25 (brs, 1H, OH) ppm; ^{13}C-NMR (100 MHz, DMSO-d$_6$): δ = 60.3, 66.4, 76.9, 105.1, 115.6, 121.7, 124.7, 128.8, 129.2, 130.1, 131.3, 132.3, 135.4, 143.7, 145.6, 154.8, 164.1, 177.2 ppm; elemental analysis for $C_{20}H_{17}Cl_2NO_4$: found: C, 59.01; H, 4.15; N, 3.33%; calculated: C, 59.13; H, 4.22; N, 3.45%.

3.4.24. 3-((3,5-Dichlorophenyl)(morpholino)methyl)-4-hydroxy-2*H*-chromen-2-one (A24). Yield: 89% (0.362 mg), white solid, m.p.: 196–198 °C;^{1}H-NMR (400 MHz, DMSO-d$_6$): δ = 2.94–3.98 (m, 8H), 5.80 (s, 1H), 7.42 (t, J = 8.4 Hz, 1H), 7.49 (d, J = 8.4 Hz, 1H), 7.75–7.90 (m, 5H), 8.11 (s, 1H) ppm; ^{13}C-NMR (100 MHz, DMSO-d$_6$): δ = 60.3, 66.7, 75.7, 105.0, 115.7, 121.4, 124.3, 129.8, 130.1, 131.4, 133.3, 134.8, 142.7, 155.0, 164.3, 176.6 ppm; elemental analysis for $C_{20}H_{17}Cl_2NO_4$: found: C, 59.34; H, 4.28; N, 3.36%; calculated: C, 59.13; H, 4.22; N, 3.45%.

3.5. *In silico* physicochemical parameters and ADMET profiling calculations

The physicochemical properties and drug-likeness studies of all α-benzyl amino coumarin compounds were obtained and evaluated for ADMET characteristics under Lipinski's rule of five and Veber rules by using SwissADME online software, the preADMET online server (**https://preadmet.webservice.bmdrc.org/**) and admetSAR (**http://lmmd.ecust.edu.cn/admetsar2/**) online server.

4. Conclusion

In summary, we have demonstrated an elegant and environmentally friendly protocol for the synthesis of α-benzyl amino coumarin derivatives by using barium silicate nanoparticles as a catalyst and water as a green solvent. Compared with other methods in existence, our method provides the advantages of better yields, inexpensive operation, cleaner reaction profile, and environmental friendliness. The *in silico* ADMET analysis performed within this study indicated that all synthesized compounds are in agreement with Lipinski's and Veber's rules. Also, the results of toxicity risk assessment tests showed that none of the compounds exhibit a risk of mutagenicity, tumorigenicity, irritation, or acute oral toxicity which highlights their potential as ideal chemotherapeutic agents.

Conflicts of interest

There are no conflicts to declare.

Acknowledgements

We are thankful to the Najafabad Branch, Islamic Azad University research council, and Shiraz University of Medical Sciences grant number 24994, for partial support of this research.

References

1 M. E. Riveiro, N. De Kimpe, A. Moglioni, R. Vazquez, F. Monczor, C. Shayo, *et al.*, Coumarins: old compounds

with novel promising therapeutic perspectives, *Curr. Med. Chem.*, 2010, **17**(13), 1325–1338.

2 Y. B. Yousif, S. Sanaa, A. Talal and A. Shtywy, Structure-activity relationships regarding the antioxidant effects of the flavonoids on human erythrocytes, *Nat. Sci.*, 2012, **4**(9), 740–747.

3 K. Abou-Melha and H. Faruk, Bimetallic complexes of schiff base bis-[4-hydroxycuomarin-3-yl]-1N, 5N-thiocarbohydrazone as a potentially dibasic pentadentate ligand. Synthesis, spectral, and antimicrobial properties, *J. Iran. Chem. Soc.*, 2008, **5**(1), 122–134.

4 C.-C. Chiang, J.-F. Mouscadet, H.-J. Tsai, C.-T. Liu and L.-Y. Hsu, Synthesis and HIV-1 integrase inhibition of novel bis-or tetra-coumarin analogues, *Chem. Pharm. Bull.*, 2007, **55**(12), 1740–1743.

5 A. A. Patel, H. B. Lad, K. R. Pandya, C. V. Patel and D. I. Brahmbhatt, Synthesis of a new series of 2-(2-oxo-2H-chromen-3-yl)-5H-chromeno [4, 3-b] pyridin-5-ones by two facile methods and evaluation of their antimicrobial activity, *Med. Chem. Res.*, 2013, **22**(10), 4745–4754.

6 Z. H. Chohan, A. U. Shaikh, A. Rauf and C. T. Supuran, Antibacterial, antifungal and cytotoxic properties of novel N-substituted sulfonamides from 4-hydroxycoumarin, *J. Enzyme Inhib. Med. Chem.*, 2006, **21**(6), 741–748.

7 Z. Chen, J. Bi and W. Su, Synthesis and antitumor activity of novel coumarin derivatives via a three-component reaction in water, *Chin. J. Chem.*, 2013, **31**(4), 507–514.

8 O. M. Abdelhafez, K. M. Amin, R. Z. Batran, T. J. Maher, S. A. Nada and S. Sethumadhavan, Synthesis, anticoagulant and PIVKA-II induced by new 4-hydroxycoumarin derivatives, *Bioorg. Med. Chem.*, 2010, **18**(10), 3371–3378.

9 A. Kumar, M. K. Gupta and M. Kumar, An efficient non-ionic surfactant catalyzed multicomponent synthesis of novel benzylamino coumarin derivative via Mannich type reaction in aqueous media, *Tetrahedron Lett.*, 2011, **52**(35), 4521–4525.

10 C. Mukhopadhyay, S. Rana and R. J. Butcher, Catalyst-free, one-pot, expeditious synthesis of aminoalkylnaphthols at room temperature, *Synth. Commun.*, 2012, **42**(20), 3077–3088.

11 M. Ghandi and E. Babazadeh, Expedient synthesis of novel coumarin-based sulfonamides, *J. Iran. Chem. Soc.*, 2015, **12**(3), 379–387.

12 P. Rao, S. Konda, J. Iqbal and S. Oruganti, InCl3 catalyzed three-component synthesis of α-benzylamino coumarins and diketones, *Tetrahedron Lett.*, 2012, **53**(39), 5314–5317.

13 M. Anary-Abbasinejad, H. Anaraki-Ardakani, A. Saidipoor and M. Shojaee, Synthesis of 3-[(acetylamino)(aryl) methyl]-4-hydroxycoumarins, *J. Chem. Res.*, 2007, **2007**(9), 535–537.

14 J. Sangshetti, F. Khan, C. Kute, Z. Zaheer and R. Ahmed, One-pot three-component synthesis of 3-(α-aminobenzyl)-4-hydroxycoumarin derivatives using nanocrystalline TiO2 as reusable catalyst, *Russ. J. Org. Chem.*, 2015, **51**(1), 69–73.

15 P. Borah, P. S. Naidu and P. J. Bhuyan, Synthesis of functionalized dihydrofurocoumarin derivatives from 3-aminoalkyl-4-hydroxycoumarin, *Synth. Commun.*, 2015, **45**(13), 1533–1540.

16 S. Baghery, M. A. Zolfigol, R. Schirhagl and M. Hasani, {[1, 4-DHPyrazine][C (CN) 3] 2} as a New Nano Molten Salt Catalyst for the Synthesis of Novel Piperazine Based bis (4-hydroxy-2H-chromen-2-one) Derivatives, *Catal. Lett.*, 2017, **147**(8), 2083–2099.

17 A. Montagut-Romans, M. Boulven, M. Lemaire and F. Popowycz, 3-Methylene-2, 4-chromandione in situ trapping: introducing molecular diversity on 4-hydroxycoumarin, *RSC Adv.*, 2016, **6**(6), 4540–4544.

18 S. V. Tiwari, J. A. Seijas, M. P. Vazquez-Tato, A. P. Sarkate, K. S. Karnik and A. P. G. Nikalje, Facile synthesis of novel coumarin derivatives, antimicrobial analysis, enzyme assay, docking study, ADMET prediction and toxicity study, *Molecules*, 2017, **22**(7), 1172.

19 H. Ghafuri, B. Ghorbani, A. Rashidizadeh, M. Talebi and M. Roshani, Fe3O4@ ZrO2/SO42-: A recyclable magnetic heterogeneous nanocatalyst for synthesis of β-amino carbonyl derivatives and synthesis of benzylamino coumarin derivatives through Mannich reaction, *Appl. Organomet. Chem.*, 2018, **32**(3), e4147.

20 N. E. Sabzi and A. Kiasat, β-Cyclodextrin based nanosponge as a biodegradable porous three-dimensional nanocatalyst in the one-pot synthesis of n-containing organic scaffolds, *Catal. Lett.*, 2018, **148**(9), 2654–2664.

21 S. Kolita, L. Dutta, P. Das and P. J. Bhuyan, One-Pot Synthesis of Unsymmetrical Bis (4-Hydroxycoumarin-3-yl) methanes, *Synlett*, 2017, **28**(17), 2291–2294.

22 P. P. Ghosh and A. R. Das, Nanocrystalline and reusable ZnO catalyst for the assembly of densely functionalized 4 H-chromenes in aqueous medium via one-pot three component reactions: a greener "NOSE" approach, *J. Org. Chem.*, 2013, **78**(12), 6170–6181.

23 J. Sahoo, S. K. Mekap and P. S. Kumar, Synthesis, spectral characterization of some new 3-heteroaryl azo 4-hydroxy coumarin derivatives and their antimicrobial evaluation, *J. Taibah Univ. Sci.*, 2015, **9**(2), 187–195.

24 M. N. S. Rad, S. Behrouz, A. R. Nekoei, Z. Faghih and A. Khalafi-Nezhad, Three-component synthesis of some novel N-heterocycle methyl-O-oxime ethers, *Synthesis*, 2011, 4068–4076.

25 H. Taghrir, M. Ghashang and M. N. Biregan, Preparation of 1-amidoalkyl-2-naphthol derivatives using barium phosphate nano-powders, *Chin. Chem. Lett.*, 2016, **27**(1), 119–126.

26 L. Emami, S. Khabnadideh, Z. Faghih, A. Solhjoo, S. Malek, A. Mohammadian, *et al.*, Novel N-Substituted Isatin-Ampyrone Schiff Bases as a New Class of Antiproliferative Agents: Design, Synthesis, Molecular Modeling and in Vitro Cytotoxic Activity, *J. Heterocycl. Chem.*, 2022, 1144–1159.